PAPER

16 × 16 MIMO Testbed for MU-MIMO Downlink Transmission

Kentaro NISHIMORI[†a)], **Riichi KUDO**[††], **Naoki HONMA**[†††], ***Members***, **Yasushi TAKATORI**[††], ***Senior Member***, ***and*** **Masato MIZOGUCHI**[††], ***Member***

SUMMARY Multi-user multiple input multiple output (MU-MIMO) systems have attracted much attention as a technology that enhances the total system capacity by generating a virtual MIMO channel between a base station and multiple terminal stations. Extensive evaluations are still needed because there are many more system parameters in MU-MIMO than in single user (SU)-MIMO and the MU-MIMO performance in actual environments is still not well understood. This paper describes the features and effectiveness of a 16 × 16 MU-MIMO testbed in an actual indoor environment. Moreover, we propose a simple adaptive modulation scheme for MU-MIMO-OFDM transmission that employs a bit interleaver in the frequency and space domains. We evaluate the frequency efficiency by obtaining the bit error rate of this testbed in an actual indoor environment. We show that 16×4×4-user MU-MIMO transmission using the proposed modulation scheme achieves the frequency utilization of 870 Mbps and 1 Gbps (respective SNRs: 31 and 36 dB) with a 20-MHz bandwidth.

key words: *multiuser MIMO, adaptive modulation scheme, OFDM, eigenvalue, bit interleaver*

1. Introduction

The growing popularity of mobile phone systems and wireless LANs has set the demand for achieving broadband wireless transmission within a limited frequency band. Multiple input multiple output-orthogonal frequency division multiplexing (MIMO-OFDM) systems have been developed because they promise to increase the channel capacity compared to single input single output (SISO) systems [1]–[4]. Moreover, multi-user MIMO (MU-MIMO) systems have recently attracted much attention as a technology that enhances the total system capacity by generating a large virtual MIMO channel between a base station and multiple terminal stations [5], [6].

Many previous studies concerning MU-MIMO systems focused on the theoretical derivation of the channel capacity [7] and performance evaluation based on computer simulations [6]. Several downlink beamforming methods and scheduling algorithms were proposed for MU-MIMO systems [8]–[12].

In order to incorporate MU-MIMO technologies into commercial systems, many system parameters must be determined. The optimal transmission control methods and antenna configurations are complex in comparison to those for single user (SU)-MIMO applications. The scheduling algorithm, which determines the number of data streams per user and the allowed number of simultaneously communicating users, largely depends on factors such as the propagation environment, the number of connected users, and the number of transmitter and receiver antennas. However, the performance of MU-MIMO technologies considering actual system parameters is not well understood.

In this paper, we describe a MU-MIMO testbed that can be used to evaluate a maximum of 16 × 16 MIMO transmissions. This testbed deals with OFDM signals according to the IEEE802.11a standard format [13], and it can be used to evaluate various system parameters such as the number of antennas, users, transmission control methods, and scheduling algorithms. In this paper, we first describe the hardware configuration and communication flow of the developed testbed.

In order to actualize the downlink beamforming scheme, an adequate modulation scheme must be implemented according to the transmission quality for each data stream. The optimal modulation scheme and coding rate for each subcarrier are ideally determined when the OFDM transmission with error correction is considered. However, the calculation complexity level increases when trying to achieve the ideal adaptive modulation strategy. Hence, we propose a simple adaptive modulation scheme for MU-MIMO-OFDM transmission that employs a bit interleaver in the frequency and space domains. The proposed scheme enables efficient adaptive modulation by calculating the effective number of eigenvalues and preparing the relationship between the average Signal to Noise Ratio (SNR) of the effective eigenvalues and the pairs comprising the modulation scheme and coding rate.

Finally, we show the experimental results in an actual indoor environment in order to evaluate the frequency utilization for a downlink beamforming scheme that is implemented in the MU-MIMO testbed. We clarify that the MU-MIMO transmission using the simple adaptive modulation scheme achieves the frequency utilization of 43.5 bits/s/Hz (870 Mbps) and 50 bits/s/Hz (1 Gbps) when the SNRs are 31 and 36 dB, respectively.

The rest of this paper is organized as follows. Section 2 outlines the 16×16 MU-MIMO testbed. The measure-

Manuscript received May 20, 2009.
Manuscript revised September 23, 2009.

[†]The author is now with the Faculty of Engineering, Niigata University, Niigata-shi, 950-2102 Japan.
[††]The authors are with NTT Network Innovation Laboratories, NTT Corporation, Yokosuka-shi, 239-0847 Japan.
[†††]The author is now with the Faculty of Engineering, Iwate University, Morioka-shi, 020-8551 Japan.
a) E-mail: nishimori@m.ieice.org

DOI: 10.1587/transcom.E93.B.345

ment conditions and proposed adaptive modulation scheme are described in Sect. 3. Section 3 also presents experimental results on the frequency utilization using the MU-MIMO testbed.

2. Configuration of 16 × 16 MU-MIMO Testbed

2.1 Hardware Configuration

The configuration of the experimental testbed for the MU-MIMO-OFDM transmission is shown in Fig. 1. The main parameters are given in Table 1. The center frequency of this testbed is 4.85 GHz. To evaluate the effect of the number of antennas and users in the MU-MIMO channels, the total numbers of transmitters and receivers are 16, respectively. The 16 × 16 MU-MIMO-OFDM transmission can be evaluated using a bandwidth of 100 MHz at maximum. Although the MU-MIMO scenario in Fig. 1 represents the case in which there are four receiver antennas and four users, it should be noted that various combinations for the number of antennas and users for both transmitters and receivers can be evaluated in this testbed. For example, if the number of receiver antennas per user is set to two, then we can deal with MU-MIMO transmission for eight users.

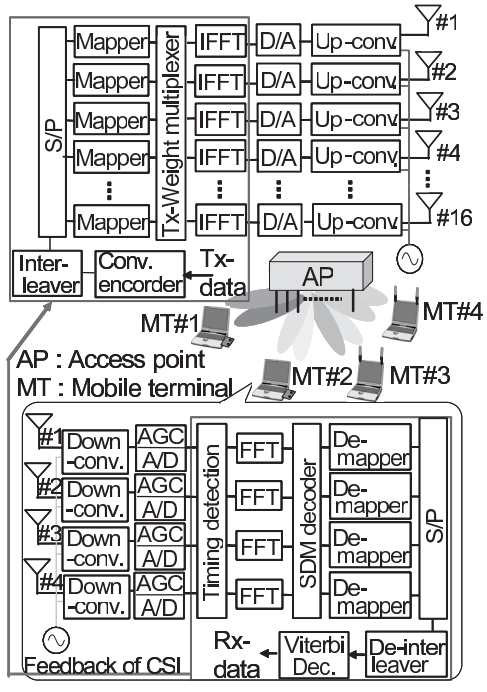

Fig. 1 Block diagram of 16 × 16 MU-MIMO testbed.

Table 1 RF parameters.

Number of Tx antennas	16
Number of Rx antennas	16
Radio frequency	4.85 GHz
Bandwidth	100 MHz (Max)
Range of AD/DA	12 bits
Transmit power	10 W (Max)
Sensitivity	−20 ∼ −70 dBm

2.2 Communication Flow

The communication flow of this testbed is described in this subsection. Table 2 represents the signal parameters that are used in this study. The frame format is shown in Fig. 2. At the transmitter, we employ convolutional coding with the constraint length of seven. These bits are interleaved for both data steams and subcarriers, and divided into streams corresponding to the modulation scheme. Next, these bits are modulated and multiplied with the transmission weight vectors. Each stream uses the same modulation scheme over all the sub-carriers. Inverse Fast Fourier transform (IFFT) blocks transform each signal into a time-domain waveform, and guard intervals (GIs) are added to mitigate the effect of multipath fading. The output signals of the IFFT are converted into analog signals and up-converted to RF signals.

At the receiver, the received RF signals are down-converted to baseband signals. Next, the baseband signals are converted into digital signals using automatic gain control (AGC) and an A/D converter. Symbol timing detection and automatic frequency control (AFC) are performed for each received preamble and the FFT is applied to the residual signals after the GIs are removed. After the FFT processing, the channel matrix is estimated by the known preambles in Fig. 2, and the data symbols are decoded using the Zero Forcing (ZF) algorithm. The demodulated bits are then serialized and de-interleaved. Finally, the Viterbi decoder estimates the transmitted bits. The frame format is based on the IEEE802.11a standard [13], which is used for commercial wireless LANs, but is extended to enable MU-MIMO-OFDM transmission. As shown in Fig. 2, each

Table 2 Signal parameters in measurement.

Sampling rate	20 MHz (A/D), 40 MHz (D/A)
Number of FFT points	64
Number of subcarriers	48 (Information)+4 (Pilot)
Symbol length	3.2 μs+0.8 μs (GI)
Preamble length	8.0 μs (short), 16.0 μs (long)
Modulation scheme	QPSK, 16QAM 64QAM, 256QAM 1024QAM
Coding rate	1/2, 2/3, 3/4, 5/6, 7/8

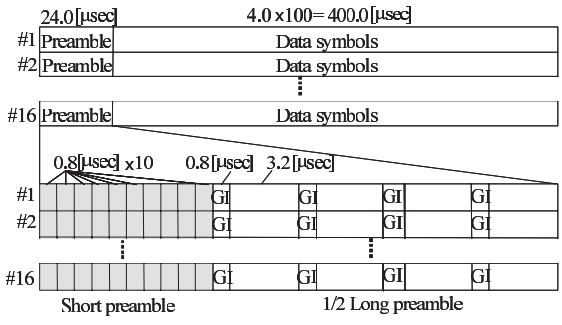

Fig. 2 Frame format of MU-MIMO testbed.

long preamble is one half the length of the 802.11a standard and transmitted in four OFDM symbol timings. In the data sequence, 100 OFDM symbols are transmitted per packet. The channel matrices at all sub-carriers are fed back to the transmitter using a cable (TCP-IP). Hence, the channel state information (CSI) can be assumed to be ideally fed back from the receiver to transmitter in this testbed.

2.3 Transmit Beamforming Method

In this paper, we use the block-diagonalization (BD) algorithm, which is well known as a practical linear beamforming method for MU-MIMO systems [9], [10]. We consider the downlink transmission. The numbers of transmit and receive antennas are assumed to be N_T and N_R, respectively. The received signal, $\mathbf{y}_i \in \mathbb{C}^{N_T \times 1}$, for User i is written as

$$\mathbf{y}_i = \mathbf{H}_i \sum_{i=1}^{N_U} \mathbf{W}_i \mathbf{x}_i + \mathbf{n}_i \tag{1}$$

where $\mathbf{H}_i \in \mathbb{C}^{N_R \times N_T}$ is the channel matrix for User i. Terms $\mathbf{x}_i$ and $\mathbf{n}_i$ are the transmit signal and noise for User i, respectively. Term N_U represents the number of users. To avoid interference, singular value decomposition (SVD) $\mathbf{H}_i^{'}$ is performed as

$$\begin{aligned}\mathbf{H}_i^{'} &= \left(\mathbf{H}_1^T \cdots \mathbf{H}_{i-1}^T \ \ \mathbf{H}_{i+1}^T \cdots \mathbf{H}_{N_U}^T\right)^T \\ &= \mathbf{U}_i^{'}(\mathbf{D}_i^{'} \ \ \mathbf{0})(\bar{\mathbf{V}}_i^{'} \ \ \tilde{\mathbf{V}}_i^{'})^H,\end{aligned} \tag{2}$$

where $\mathbf{H}_i^{'}$ is the total channel matrix except for $\mathbf{H}_i$. Term $\bar{\mathbf{V}}_i^{'}$ represents the signal space of all users except User i. Term $\tilde{\mathbf{V}}_i^{'}$ represents the null space weight that does not interfere with User i. In the BD algorithm, the virtual transmission weights are calculated using the SVD for the null space channel matrix, $\mathbf{H}_i\tilde{\mathbf{V}}_i^{'}$, as

$$\mathbf{H}_i\tilde{\mathbf{V}}_i^{'} = \mathbf{U}_i^{''}\mathbf{D}_i^{''}\mathbf{V}_i^{''H} \tag{3}$$

where $\mathbf{D}_i^{''} \in \mathbb{C}^{N_R \times N_R}$ is the diagonal matrix and the diagonal elements of $\mathbf{D}_i^{''}$ are the square root of the eigenvalues of $\mathbf{H}_i\tilde{\mathbf{V}}_i^{'}\tilde{\mathbf{V}}_i^{'H}\mathbf{H}_i^H$, $\lambda_{i,1}^{'}$, $\lambda_{i,2}^{'}$, $\cdots$, $\lambda_{i,N_R}^{'}$. The transmission weight matrices for User i, $\mathbf{W}_i^{'}$, are determined as $\tilde{\mathbf{V}}_i^{'}\bar{\mathbf{V}}_i^{''}$ and the transmission qualities of data streams correspond to the diagonal elements of $\mathbf{D}_i^{''}$.

3. Performance Evaluation of MU-MIMO Testbed

3.1 Measurement Environment

In order to clarify the characteristics of the proposed MU-MIMO testbed in terms of the proposed modulation scheme, we conducted measurements in an indoor environment. The measurement environment is shown in Fig. 3. The measurement space in the room is $17.6 \times 12.1 \times 3$ [m]. Sleeve antennas are used for the transmitter and receiver antennas. Linear arrays are used for the transmitter and receiver arrays. The element spacing for the transmitter and that for the receiver antennas are 1.0 and 0.5 wavelengths, respectively.

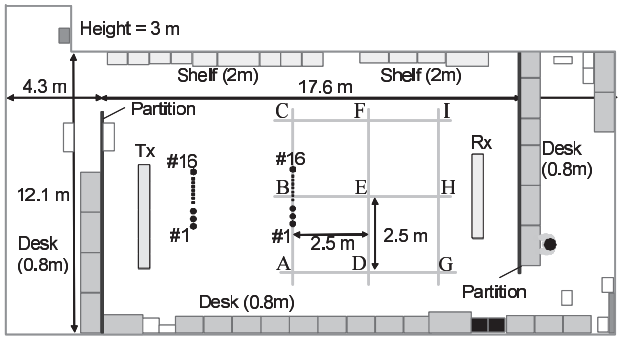

Fig. 3 Measurement environment.

The heights of the transmitter and receiver antennas are 1.7 and 0.7 m, respectively. The maximum transmission power per antenna is −6 dBm.

The transmitter antennas are located at Point Tx and the receiver antennas are located at nine points (Rx-A to I). All users are assumed to be located at each receiving point in order to employ the evaluation among the users whose SNRs are almost the same. To clarify the dependency of the transmission quality on the direction of the receiver array antenna, we evaluate three rotation angles (−45°, 0°, and 45°) at each receiving point. Two to eight user cases are assumed in the MU-MIMO scenario. The bit error rate (BER) and frequency utilization for two to eight receiver antennas are given when the MU-MIMO scheme is evaluated with transmit beamforming based on the BD algorithm described in Sect. 2.3. We use the ZF algorithm, which is well known as the SDM decoding method. We also evaluate the Eigen-mode transmission [14]–[15] when considering the SU-MIMO transmission [16].

In this measurement, we use the modulation signals given in Table 2 and the frame format in Fig. 2. In this measurement, we use the modulation signals given in Table 2. The total number of bits ranges from 10^7 to 10^8 and the frequency utilization is obtained at the BER of 10^7 to 10^8 bits. The frequency utilization (2.7 bits/s/Hz or 54 Mbit/s per 20 MHz) is evaluated for the 64QAM modulation scheme with the coding rate of R = 3/4, according to the IEEE802.11a standard. In this case, 4.5 bits per subcarrier per OFDM symbol are transmitted.

3.2 Simple Adaptive Modulation Scheme

In this subsection, simple adaptive modulation and coding is proposed. Figure 4 shows the distribution of eigenvalues that are obtained using the BD algorithm in Sect. 2.3. The eigenvalue distribution is shown when an i.i.d. channel is assumed in the propagation environment. For this calculation, 10,000 trials are performed. Figure 4 shows the results when the number of antennas (N_R) per user is 3 or 4, and when the number of transmitter antennas (N_T) and the number of users (N_U) are 16 and 4, respectively.

Figure 4 shows that the fourth eigenvalue is very small compared to the other eigenvalues in the 16×4×4-user case,

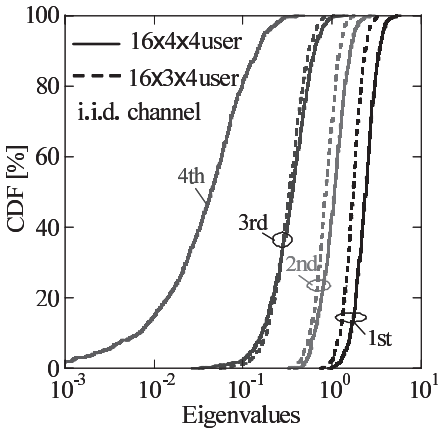

Fig. 4 Eigenvalue distribution when using BD algorithm.

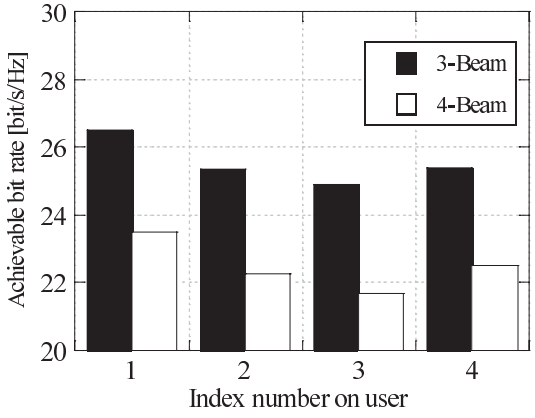

Fig. 5 Achievable bit rate comparison (3 and 4 beams).

while the third eigenvalue is not small in the $16 \times 3 \times 4$-user case. Moreover, since the range of the fourth eigenvalue exceeds 20 dB, it is very difficult to assign a single modulation scheme for such a data stream.

Figure 5 shows a comparison of the achievable bit rate based on the BD algorithm [10] using the channel matrix, when three or four beams are assumed for each user. The channel matrixes for $16 \times 4 \times 4$-user and $16 \times 3 \times 4$-user are measured at Rx-A to I in Fig. 3 and the achievable bit rate is calculated by using the channel matrix for each receiving point. The achievable bit rate in Fig. 5 is averaged by the results on all subcarriers and receiving points (Rx-A to I in Fig. 3). Note that the achievable bit rate is different from the frequency utilization obtained by the actual data transmission because the achievable bit rate is determined using the eigenvalues that are obtained in Eq. (3). Figure 5 shows that a higher achievable bit rate with three beams is obtained compared to that with four beams for all users. Hence, the fourth eigenvalue is not useful from the viewpoint of the channel capacity.

Figure 6 represents the flow of the proposed scheme. Based on the results in Figs. 4 and 5, we first discard the eigenvalues that are less than the threshold value in the proposed scheme (Step 1 in Fig. 6). The eigenvalues for all

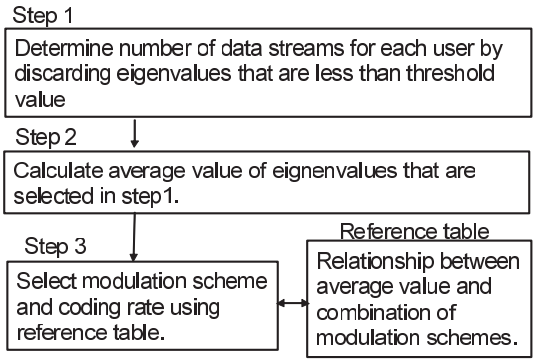

Fig. 6 Flow of adaptive modulation scheme.

Table 3 Example of relationship between averaged eigenvalue and combination of modulation schemes (R=5/6).

Mod. scheme 1	Mod. scheme 2	Mod. scheme 3	$\bar{\lambda}$ [dB]
1024QAM	1024QAM	256QAM	$33 < \bar{\lambda} < 37$
1024QAM	256QAM	256QAM	$31 < \bar{\lambda} < 37$
1024QAM	256QAM	64QAM	$30 < \bar{\lambda} < 37$
1024QAM	256QAM	16QAM	$27.5 < \bar{\lambda} < 34$
256QAM	256QAM	64QAM	$27.5 < \bar{\lambda} < 32$
256QAM	64QAM	64QAM	$26 < \bar{\lambda} < 32$
256QAM	64QAM	16QAM	$25.0 < \bar{\lambda} < 29$
64QAM	64QAM	64QAM	$25.0 < \bar{\lambda} < 29$
64QAM	64QAM	16QAM	$22.5 < \bar{\lambda} < 26.5$
64QAM	16QAM	16QAM	$20 < \bar{\lambda} < 26$
64QAM	16QAM	QPSK	$18 < \bar{\lambda} < 22.5$
16QAM	16QAM	QPSK	$16 < \bar{\lambda} < 21.5$
16QAM	QPSK	QPSK	$13 < \bar{\lambda} < 19$
QPSK	QPSK	QPSK	$12 < \bar{\lambda} < 16.5$

subcarriers are checked. In this paper, we set this threshold value to 0 dB, which means an internal noise power. On the other hand, employing an interleaver in both data streams and subcarriers suppresses the degradation in the transmission quality for subcarriers with a low SNR, even if fixed modulation schemes are employed for each subcarrier on the data streams corresponding to the first to third eigenvalues.

As the next step, we calculate the average value of the eigenvalues that are selected in Step 1 (Step 2 in Fig. 6). The eigenvalue is averaged by using those for all subcarriers. Table 3 shows an example of the relationship between the average eigenvalue and the combination of the modulation schemes when coding rate R is 5/6. Table 3 is obtained by the combination of modulation schemes that achieves error-free transmission for a certain SNR. The number of trials is 1000 and the i.i.d. channel is assumed in this calculation when changing the SNR.

In OFDM systems, the optimal method is to select the modulation scheme and coding rate based on the eigenvalue for each subcarrier. However, the selection method is

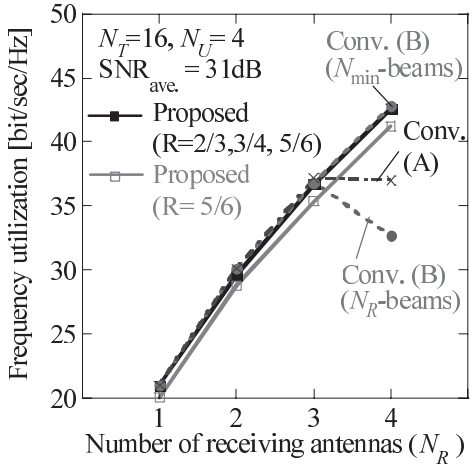

Fig. 7 Frequency utilization versus number of receiver antennas (N_T = 16, N_U = 4).

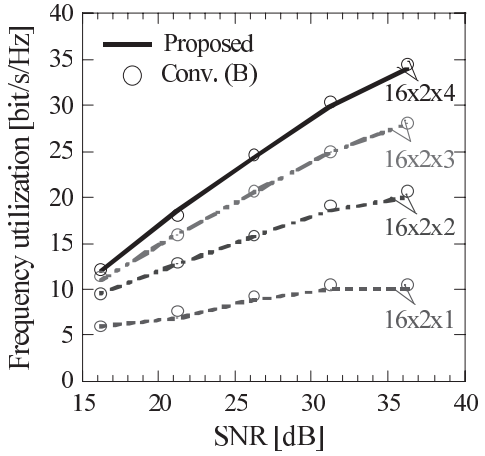

Fig. 8 Frequency utilization versus SNR when N_R is two.

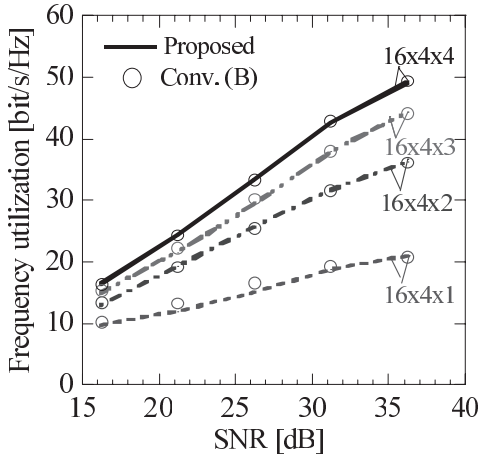

Fig. 9 Frequency utilization versus SNR when N_R is four.

very complex in such a scheme, because many combinations must be considered for each eigenvalue. On the contrary, the key point here is that we utilize the average eigenvalue using those for all subcarriers, which represents the transmission quality when considering the interleaver for the data streams and subcarriers. Since the interleaver can mitigate the degradation in the transmission quality for the subcarriers with a low SNR, different modulation schemes and coding rates for each subcarrier are not required and the average SNR or average eigenvalue approximately represents the transmission quality. If we prepare a database such as Table 3 in advance, appropriate modulation schemes for each data stream can be easily determined. As shown in Step 3 in Fig. 6, the modulation scheme and coding rate are selected by using the reference table. Actually, we prepare the reference tables for each coding rate and the number of beams in advance.

3.3 Effectiveness of MU-MIMO Downlink Transmission

First, we clarify the effectiveness of the proposed adaptive modulation and coding scheme as shown in 3.2. Figure 7 shows the frequency utilization versus the number of receiver antennas (N_R) when the numbers of transmitter antennas (N_T) and users (N_U) are 16 and 4, respectively. We compare the results between the proposed modulation scheme and the conventional schemes. In conventional scheme (A), the modulation scheme and coding rate are determined according to each SNR for each subcarrier. Conventional scheme (B) means that all possible combinations of modulation schemes where the BER becomes zero are checked using the channel matrix. $N_{\min}$ equals $\min(N_R, 3)$.

Figure 7 shows that the frequency utilization with the proposed adaptive modulation scheme becomes almost the same as that for conventional scheme (B) when N_R is less than four, although the calculation complexity of the proposed scheme is dramatically reduced compared to conventional scheme (B). Surprisingly, the frequency utilization when N_R is four is decreased compared to that when N_R is three, if the number of selected beams is fixed to four in conventional scheme (B). Hence, we found that the minimum eigenvalue significantly affects the degradation in the MU-MIMO transmission when N_T equals $N_R \times N_U$. Moreover, even if the modulation and coding are assigned based on each subcarrier (conventional scheme (A)), the frequency utilization is not improved when N_R equals four because the fourth eigenvalue is not useful as shown in Fig. 6. On the other hand, the frequency utilization of the proposed scheme is almost the same compared to that for conventional scheme (B) when the number of selected beams is set to three.

Figures 8 and 9 indicate the frequency utilization versus the SNR when the number of receiver antennas is two and four, respectively. In these figures, the proposed adaptive modulation scheme is employed. The frequency utilization is defined as the transmission bit rate at which the BER is less than 10^{-7}. Figures 8 and 9 show that the frequency utilization can be improved due to the increase in the number of users and the SNR. For example, the frequency utilization for 43.5/50 and 30/35 bits/s/Hz (SNR: 31/36 dB) can be obtained when $16 \times 4 \times 4$-user and $16 \times 2 \times 4$ user MU-MIMO transmission are employed, respectively. More-

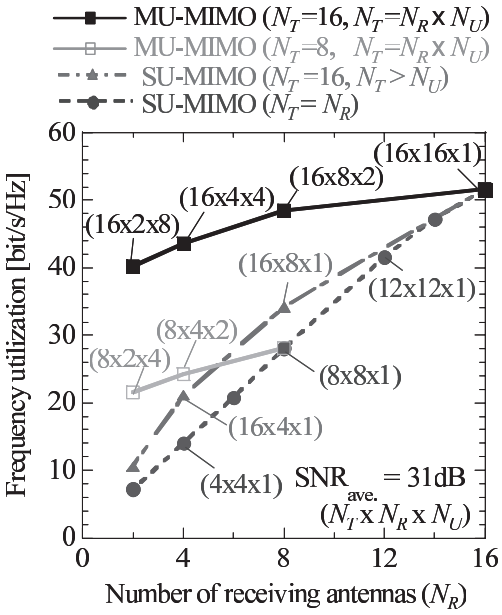

Fig. 10 Frequency utilization comparison between MU-MIMO and SU-MIMO.

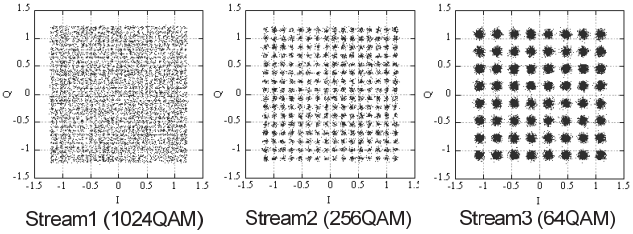

Fig. 11 Example of signal constellations (N_T = 16, N_R = 4, N_U = 4).

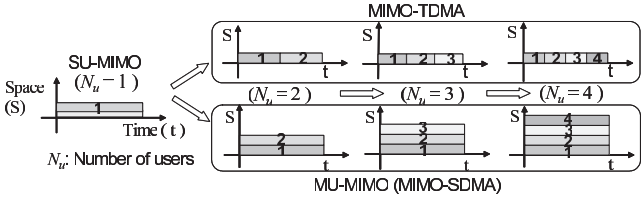

Fig. 12 Resource allocations for MIMO-TDMA and MU-MIMO.

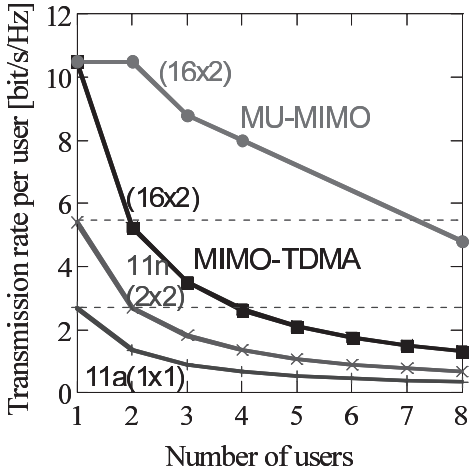

Fig. 13 Transmission rate that can be assigned to one user.

over, Figs. 8 and 9 show that the frequency utilization with the proposed adaptive modulation scheme becomes almost the same as that for conventional scheme (B) when N_R is less than four.

Next, we compare the difference in improvement for the MU-MIMO transmission when the number of receiver antennas is changed. Figure 8 shows that the frequency utilization of MU-MIMO transmission is 2.0 to 3.3 times higher compared to the eigenvector beamforming method in SU-MIMO, when the number of receiver antennas is 2. On the other hand, the frequency utilization of MU-MIMO transmission becomes 1.6 to 2.4 times higher compared to SU-MIMO, when the number of receiver antennas is 4. Thus, we found that the effect on MU-MIMO is obtained with a smaller number of antennas.

We compare the frequency utilization between MU-MIMO and SU-MIMO in Fig. 10, when the number of receiver antennas (N_R) is changed. For the MU-MIMO scenario, we set the condition where N_T equals $N_R \times N_U$. The average SNR is 31 dB. We employ the proposed modulation scheme in this figure. Figure 10 shows that the frequency utilization with the SU-MIMO transmission cannot be significantly improved when N_T is greater than N_R. On the other hand, a frequency utilization of over 40 bits/s/Hz can be obtained using the MU-MIMO transmission (N_T = 16) using the proposed modulation scheme, even if the number of receiver antennas is 2.

Figure 11 shows signal constellation examples of the 16 × 4 × 4-user transmission. As shown in Fig. 11, the MU-MIMO transmission using our testbed enables even 1024QAM transmission. In this example, frequency utilization of 48 bits/s/Hz was obtained by 16 × 4 × 4-User MU-MIMO transmission, when the SNR is 35 dB.

Finally, we evaluate the transmission rate that can be assigned to one user. Figure 12 shows the considered scenario for this evaluation. The results are shown in Fig. 13. When considering SU-MIMO transmission, we assume that time division multiple access is applied for each user in SU-MIMO scheme. Moreover, we assume that the time resources allocated fairly to each user as shown in Fig. 12. Hence, the frequency utilization for each user in the SU-MIMO scheme in Fig. 13 becomes $1/N_U$ of that for a one user case when the number of users is N_U. For comparison, the *maximum* frequency utilization for SISO and 2 × 2 MIMO using IEEE802.11a and n are shown in Fig. 13. In the case of SISO in IEEE802.11a, the frequency utilization is 2.7 bit/s/Hz without multiple access when employing 64QAM and R = 3/4. For the 2 × 2 MIMO transmission [13], the transmission with 2 streams (64QAM and coding rate, R = 3/4) is assumed and the frequency utilization is 5.4 bit/s/Hz.

Figure 13 shows that the frequency utilization with N_U-user transmission does not become $1/N_U$ of that with one

user transmission when applying MU-MIMO transmission. More specifically, the transmission rate for one user can be improved by using MU-MIMO transmission compared to SU-MIMO transmission using the TDMA scheme. For example, the transmission rate per user in 16×2 MIMO is almost the same as that for 2×2 MIMO with only one user transmission, when 2 users are considered in the TDMA scheme. On the other hand, the transmission with 16×2 MU-MIMO can guarantee the transmission rate obtained by 2×2 MIMO up to 6 to 7 users.

4. Conclusion

This paper described a MU-MIMO testbed that deals with 16×16 MIMO-OFDM transmission. We also proposed a simple adaptive modulation scheme that employs a bit interleaver for the data streams and subcarriers for MU-MIMO-OFDM transmission. Using this testbed, we evaluated the frequency utilization for downlink transmission in a MU-MIMO channel in an actual indoor environment. We clarified that the $16 \times 4 \times 4$-user MU-MIMO transmission using the proposed modulation scheme achieved a frequency utilization of over 43.5/50 bits/s/Hz (0.87/1 Gbps) when the SNR was 31 and 36 dB, respectively. The frequency utilization of the MU-MIMO transmission with four users is 2.4 to 3.3 times higher compared to the eigenvector beamforming method in SU-MIMO when the number of transmitter antennas is fixed to 16 and the number of receiver antennas is changed from 2 to 4. Moreover, we clarified the effectiveness of MU-MIMO transmission compared to TDMA based MIMO when considering the transmission rate per user. We found that the transmission with 16×2 MU-MIMO can guarantee the transmission rate obtained by 2×2 IEEE802.11n based MIMO up to 6 to 7 users.

A user selection scheme is required in MU-MIMO systems, although we did not focus on it in this paper. An important future investigation topic is to evaluate user selection for users with different SNRs in order to enhance the reliability of MU-MIMO transmission in actual environments.

Acknowlegement

The part of this work is supported by the Ministry of Internal Affairs and Communications, Japan, under the grant, "Research and development of fundamental technologies for advanced radio frequency spectrum sharing in mobile communication systems." The authors thank Mr. Masaaki Ida, and Mr. Yoshinobu Makise for their help on the indoor measurement.

References

[1] G.J. Foschini and M.J. Gans, "On limits of wireless communications in a fading environment when using multiple antennas," Wirel. Pers. Commun., vol.6, pp.311–335, 1998.
[2] G.L. Stuber, J.R. Barry, S.W. Mclaughlin, Y. Li, M.A. Ingram, and T.G. Pratt, "Broadband MIMO-OFDM wireless communications," Proc. IEEE, vol.92, pp.271–294, Feb. 2004.
[3] "MIMO implementation aspects," IEEE Radio and Wireless Conference (RAWCON), Workshop WS2, Sept. 2004.
[4] A. Paulraj, R. Nabar, and D. Gore, Introduction to Space-Time Wireless Communications, Cambridge University Press, 2003.
[5] R.H. Roy, "Spatial division multiple access technology and its application to wireless communication systems," Proc. IEEE VTC 1997, vol.2, pp.730–734, May 1997.
[6] Q.H. Spencer, C.B. Peel, A.L. Swindlehurst, and M. Haardt, "An introduction to the multi-user MIMO downlink," IEEE Commun. Mag., vol.42, no.10, pp.60–67, Oct. 2004.
[7] A. Goldsmith, S.A. Jafar, N. Jindal, and S. Vishwanath, "Capacity limits of MIMO channels," IEEE J. Sel. Areas Commun., vol.21, no.5, pp.684–702, June 2003.
[8] R.L. Choi, M.T. Ivrlac, R.D. Murch, and J.A. Nossek, "Joint transmit and receive multi-user MIMO decomposition approach for the downlink of multi-user MIMO systems," Proc. IEEE VTC 2003-Fall, vol.1, pp.409–413, Oct. 2003.
[9] K.K. Wong, R.D. Murch, and K.B. Letaief, "A joint-channel diagonalization for multiuser MIMO antenna systems," IEEE Trans. Wirel. Commun., vol.2, no.4, pp.773–786, July 2003.
[10] Q.H. Spencer, A.L. Swindlehurst, and M. Haardt, "Zero forcing methods for downlink spatial multiplexing in multiuser MIMO channels," IEEE Trans. Signal Process., vol.52, no.2, pp.461–471, Feb. 2004.
[11] M. Fuchs, G.D. Galdo, and M. Haardt, "A novel tree-based scheduling algorithm for the downlink of multi-user MIMO systems with ZF beamforming," Proc. IEEE ICASSP'05, vol.3, pp.1121–1124, March 2005.
[12] M. Airy, S. Shakkattai, and R.W. Heath, Jr., "Spatially greedy scheduling in multi-user MIMO wireless systems," Conference Record of the Thirty-Seventh Asilomar Conference, vol.1, pp.982–986, Nov. 2003.
[13] IEEE802.11.a, "High speed physical layer (PHY) in 5 GHz band," 1999.
[14] J.B. Andersen, "Array gain and capacity for known random channels with multiple element arrays at both ends," IEEE J. Sel. Areas Commun., vol.18, no.11, pp.2172–2178, Nov. 2000.
[15] K. Miyashita, T. Nishimura, T. Ohgane, Y. Ogawa, Y. Takatori, and K. Cho, "High data-rate transmission with Eigenbeam Space Division Multiplexing (E-SDM) in a MIMO channel," Proc. IEEE VTC2002-Fall, vol.3, pp.1302–1306, 2002.
[16] R. Kudo, K. Nishimori, Y. Takatori, and K. Tsunekawa, "Experimental evaluation of eigenvector beamforming method with 8×4 MIMO-OFDM testbed," Proc. IEEE VTC 2006-Spring, May 2006.

Kentaro Nishimori received the B.E., M.E. and Dr.Eng. degrees in electrical and computer engineering form Nagoya Institute of Technology, Nagoya, Japan in 1994, 1996 and 2002, respectively. In 1996, he joined the NTT Wireless Systems Laboratories, Nippon Telegraph and Telephone Corporation (NTT), in Japan. He was senior research engineer on NTT Network Innovation Laboratories. He is now an associate professor in Niigata University. He was a visiting researcher at the Center for Teleinfrastructure (CTIF), Aalborg University, Aalborg, Denmark in 2006. He is currently an editor for the Transactions on Communications for the IEICE Communications Society and Assistant Secretary of Technical Committee on Antennas and Propagation of IEICE. He received the Young Engineers Award from the IEICE of Japan in 2001, Young Engineer Award from IEEE AP-S Japan Chapter in 2001, Best Paper Award of Software Radio Society in 2007 and Distinguished Service Award from the IEICE Communications Society in 2005 and 2008. His current research interest is Multi-user MIMO systems and cognitive radio systems. He is a member of IEEE.

Riichi Kudo received the B.S. and M.S. degree in geophysics from Tohoku University, Japan, in 2001 and 2003, respectively. In 2003, he joined NTT Network Innovation Laboratories, Yokosuka, Japan. He has been engaged in the MIMO communication systems and the beamforming method. He received the Young Engineer Award from the Institute of Electronics, Information and Communication Engineers (IEICE) Japan in 2006. His current research interest is digital signal processing for wireless and optical communication systems. He is a member of IEEE.

Naoki Honma received the B.E., M.E., and Ph.D. degrees in electrical engineering from Tohoku University, Sendai, Japan in 1996, 1998, and 2005, respectively. From 1998 to 2009, he was with the NTT Radio Communication Systems Laboratories, Nippon Telegraph and Telephone Corporation (NTT), in Japan. He is now an Associate Professor at Iwate University. His research interest includes compact antennas for MIMO communications, and propagation for wireless communication systems. He received the Young Engineers Award from the IEICE of Japan in 2003, the APMC Best Paper Award in 2003, and the best paper award from the IEICE Communication Society in 2006. He is a member of IEEE.

Yasushi Takatori was born in Tokyo, Japan, 1971. He received his B.E. degree in electrical and communication engineering and his M.E. degree in system information engineering from Tohoku University, Sendai, Japan in 1993 and 1995, respectively. He received his Ph.D. degree in wireless communication engineering from Aalborg University, Denmark in 2005. In 1995, he joined the Wireless Systems Laboratories, Nippon Telegraph and Telephone Corporation (NTT), in Japan. He is currently a senior research engineer in the Wireless Systems Innovation Laboratory of NTT Network Innovation Laboratories. He was a visiting researcher at the Center for TeleInFrastructure (CTIF), Aalborg University, Aalborg, Denmark from 2004 to 2005. He received the Young Engineers Award from the IEICE of Japan in 2000, the Excellent Paper Award of WPMC in 2004 and YRP Award in 2005. His current research interest is MIMO systems, spatial signal processing techniques and ultra-high speed optical communication systems. He is a member of the IEEE.

Masato Mizoguchi was born in Tokyo, Japan, in 1965. He received the B.E. and M.E. degrees in electrical engineering from Tokyo University of Science, Japan in 1989 and 1991, respectively. In 1991, he joined Nippon Telegraph and Telephone Corporation (NTT) and was mainly engaged in research and development of personal communication systems and high data rate wireless LANs including the IEEE 802.11a systems. He is currently a Senior Research Engineer, Supervisor in the Wireless Systems Innovation Laboratory of NTT Network Innovation Laboratories, where he is engaged in future wireless broadband and ubiquitous systems. He received the Young Researcher's Award in 1998, the Best Paper Award in 2000 and the Achievement Award in 2006 from IEICE. He is a member of IEEE.